Strong first-order phase transition in a rotating neutron star core and the associated energy release

J. L. Zdunik[1], M. Bejger[2,1], P. Haensel[1], and E. Gourgoulhon[2]

[1] N. Copernicus Astronomical Center, Polish Academy of Sciences, Bartycka 18, 00-716 Warszawa, Poland
  e-mail: jlz@camk.edu.pl; bejger@camk.edu.pl; haensel@camk.edu.pl
[2] LUTh, Observatoire de Paris, CNRS, Université Paris Diderot, 5 Pl. Jules Janssen, 92190 Meudon, France
  e-mail: Eric.Gourgoulhon@obspm.fr

ABSTRACT

Aims. We calculate the energy release associated with a strong first-order phase transition, from normal phase N to an "exotic" superdense phase S, in a rotating neutron star. Such a phase transition N $\longrightarrow$ S, accompanied by a density jump $\rho_{\rm N} \longrightarrow \rho_{\rm S}$, is characterized by $\rho_{\rm S}/\rho_{\rm N} > \frac{3}{2}(1 + P_0/\rho_{\rm N} c^2)$, where P_0 is the pressure at which phase transition occurs. Configurations with small S-phase cores are then unstable and collapse into stars with large S-phase cores. The energy release is equal to the difference in mass-energies between the initial (normal) configuration and the final configuration containing an S-phase core, the total stellar baryon mass and angular momentum being kept constant.
Methods. The calculations of the energy release are based on precise numerical 2D calculations. Polytropic equations of state (EOSs) as well as realistic EOSs with strong first-order phase transition due to kaon condensation are used. For polytropic EOSs, a large parameter space is studied.
Results. For a fixed "overpressure", $\delta\overline{P}$, defined as the relative excess of central pressure of a collapsing metastable star over the pressure of the equilibrium first-order phase transition, the energy release $E_{\rm rel}$ does not depend on the stellar angular momentum. It coincides with that for nonrotating stars with the same $\delta\overline{P}$. Therefore, results of 1D calculations of $E_{\rm rel}(\delta\overline{P})$ for non-rotating stars can be used to predict, with very high precision, the outcome of much harder to perform 2D calculations for rotating stars with the same $\delta\overline{P}$. This result holds also for $\delta\overline{P}_{\rm min} < \delta\overline{P} < 0$, corresponding to phase transitions overcoming the energy barrier separating metastable N-phase configurations from those with an S-phase core. Such phase transitions could be realized in the cores of newly born, hot, pulsating neutron stars.

Key words. dense matter – equation of state – stars: neutron – stars: rotation

1. Introduction

One of the mysteries of neutron stars is the structure of their superdense cores. Many theories of dense matter predict a phase transition into an "exotic" state (i.e., not observed in the laboratory). Theoretical predictions include boson condensation of pions and kaons, and deconfinement of quarks (for a review see e.g. Glendenning 2000; Weber 1999; Haensel et al. 2007).

The first-order phase transitions, accompanied by discontinuities in the thermodynamic potentials, seem to be the most interesting, as far as the the structure and dynamics of neutron stars are concerned. In the simplest case, one considers states consisting of one pure phase. High degeneracy of the matter constituents implies that the effects of temperature can be neglected. At thermodynamic equilibrium, the phase transition occurs at a well defined pressure P_0. It is accompanied by a density jump at the phase interface.

A first-order phase transition in a neutron star core is associated with the collapse of the initial metastable configurations of exclusively of non-exotic (normal – N) phase, into a more compact configuration with a core of the superdense (S) exotic phase. At the core edge the pressure is P_0, and the density undergoes a jump from $\rho_{\rm N}$ on the N-side to $\rho_{\rm S}$ on the S-side. The collapse, called "core-quake", is associated with a release of energy, $E_{\rm rel}$. A neutron star core-quake implied by a first-order phase transition in a stellar core could occur during an evolutionary process in which central pressure increases. Examples of such processes are mass accretion and pulsar spin-down. In both cases, the initial and final configurations are rotating. One assumes that the baryon mass of the collapsing star, $M_{\rm b}$, is conserved (no mass ejection) and that the total angular momentum, J, is also conserved (J loss due to radiation during a core-quake due to radiation of the electromagnetic and gravitational waves is negligible).

Crucial for the core-quake is the value of the parameter $\lambda \equiv \rho_{\rm S}/\rho_{\rm N}$. If $\lambda < \lambda_{\rm crit} \equiv \frac{3}{2}(1 + P_0/\rho_{\rm N} c^2)$, then the configurations with arbitrarily small cores of the S-phase are stable with respect to axisymmetric perturbations (Seidov 1971; Kaempfer 1981; Haensel et al. 1986; Zdunik et al. 1987). To have a core-quake in an evolving neutron star, a metastable core of the N-phase with central pressure $P_{\rm c} > P_0$ and radius $r_{\rm N}$ should form first. This core is "overcompressed", with the degree of overcompression measured by a dimensionless "overpressure" $\delta\overline{P} \equiv (P_{\rm c} - P_0)/P_0$. At some critical value of the overpressure, the S-phase nucleates, and the S-core of radius $r_{\rm s}$ forms. For $\delta\overline{P} \longrightarrow 0$, we have $r_{\rm s} \longrightarrow 0$. This is the case of a *weak first order phase transition*. Up to now, all but one numerical calculation was restricted to the spherical non-rotating neutron stars (Haensel & Prószyński 1982; Haensel et al. 1986; Zdunik et al. 1987; Haensel et al. 1990; Muto & Tatsumi 1990). An exception is the work based on precise 2D calculations performed for weak first-order phase transitions in rotating neutron stars (Zdunik et al. 2007).

For a strong first-order phase transition ($\lambda > \lambda_{\rm crit}$) in a neutron star core, $\delta\overline{P} \longrightarrow 0$ implies $r_{\rm s} \longrightarrow r_{\rm s,min}$, where $r_{\rm s,min}$ is a sizable fraction of the stellar radius. The core-quake, accompanying the phase transition, is a large-scale phenomenon, with energy release $E_{\rm rel} \sim 10^{51}$–10^{52} erg. Existing numerical calculations were restricted to spherical non-rotating neutron stars (Migdal et al. 1979; Haensel & Prószyński 1980, 1982; Kaempfer 1982; Berezin et al. 1982, 1983; Diaz Alonso 1983; Berezhiani et al. 2003).

In the present paper we calculate the energy release due to a *strong first-order phase transition* in a *rotating* neutron star. The calculations are performed using very precise 2D codes and a set of EOSs with strong first-order phase transitions. We show that similarly to the case of a weak first-order phase transition studied in Zdunik et al. (2007), the energy released during a core-quake depends only on the excess of the central pressure of the metastable configuration over P_0, and is to a very good approximation independent of the angular momentum of collapsing star. Moreover, we show that this property holds also for core-quakes with initial $P_{\rm c} < P_0$, which require additional energy needed to overcome the energy barrier.

The paper is organized in the following way. In Sect. 2 we describe the general properties of the first-order phase transitions in the stellar core with particular emphasis on the metastability and instability of neutron star cores. Analytic models of the EOSs with first-order phase transitions, allowing for very precise 2D calculations, are considered in Sect. 3.1, where we derive generic properties of the energy release due to a first order phase transition at the center of a rotating star. In Sect. 3.2 we present our results obtained for a realistic EOS of normal phase, and we confirm the remarkable properties of the energy-overpressure relation (i.e., the independence from J), obtained in the previous section. In Sect. 4 we discuss the decomposition of the energy release into kinetic and internal energies. Section 5 is devoted to the problem of transition of one phase star into stable, two phase configuration through the energy barrier. Finally, Sect. 6 contains discussion of our results and conclusion.

2. Families of neutron stars

All constituents of matter are strongly degenerate and the temperature dependence of the EOS parameters can be neglected at the densities under consideration. In what follows we will use the notation from Zdunik et al. (2007) (see the schematic Maxwell construction in Fig. 1 there); here we will focus on *strong* phase transitions only. The mechanism of nucleation to the S-phase is essentially the same as in a *weak* ($\lambda < \lambda_{\rm crit}$) phase transition. Discussion of the nucleation time $\tau_{\rm nucl}$ of the S-phase in an accreting or spinning down neutron star with increasing $P_{\rm c}$ was presented by Zdunik et al. (2007); the particular case of a hot accreting neutron star was considered by Berezhiani et al. (2003). Calculations of $\tau_{\rm nucl}$ in a dense neutron star core metastable with respect to the pion condensation were performed by Haensel & Schaeffer (1982) and Muto & Tatsumi (1990). The case of nucleation of quark matter was studied by Iida & Sato (1997, 1998), while nucleation of the kaon condensate was considered by Norsen (2002).

For a given EOS, nonrotating hydrostatic equilibrium configurations of neutron stars form a one-parameter family, the parameter being, e.g., central pressure $P_{\rm c}$. Notice, that $P_{\rm c}$ is preferred over $\rho_{\rm c}$ because the pressure is strictly continuous and monotonous in the stellar interior, while density can suffer discontinuities. For an EOS with a first order phase transition, and without allowing for metastability of the N phase, neutron
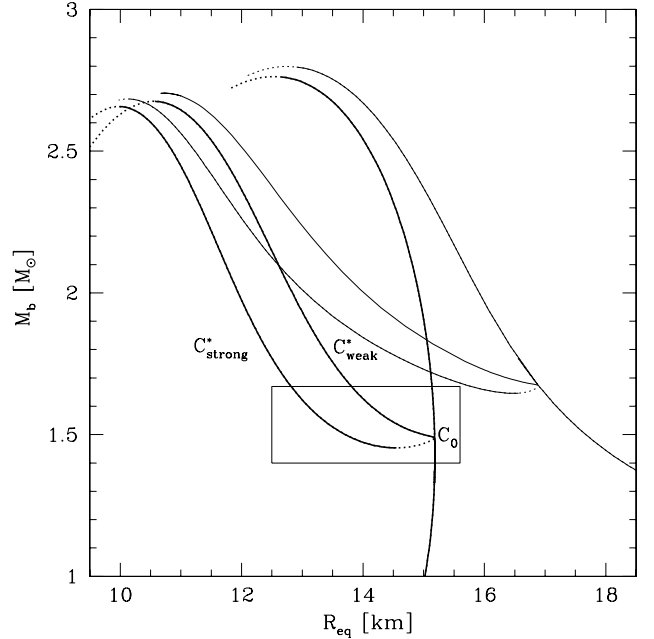

Fig. 1. Baryon mass vs. equatorial radius for hydrostatic equilibrium configurations calculated for three types of EOSs of dense matter, described in the text. Solid line – stable; dotted line – unstable configurations. Thick lines correspond to the non-rotating models, thin lines to the rigidly rotating configurations with a fixed total stellar angular momentum $J = 1.2 \times GM_\odot^2/c$.

stars form two families: a family of stars composed solely of the N-phase $\{C\}$, and a family of those having an S-phase core $\{C^\star\}$.

The configuration $\{C^\star\}$ with a small S-phase core is unstable for $\lambda > \lambda_{\rm crit} \equiv \frac{3}{2}(1 + P_0/\rho_{\rm N} c^2)$ (Seidov 1971; Kaempfer 1981; Haensel et al. 1986; Zdunik et al. 1987). Therefore, the topology of the complete set of stable hydrostatic configurations of non-rotating neutron stars, parametrized by $P_{\rm c}$, and plotted, e.g., in the mass-radius plane, depends on the value of λ. Namely, for $\lambda < \lambda_{\rm crit}$, the sum of $\{C\}$ and $\{C^\star\}$ is continuous, while for $\lambda > \lambda_{\rm crit}$ it is not (i.e., the families $\{C\}$ and $\{C^\star\}$ are disjoint). Recently, it has been shown that this property is generic for an EOS with a phase transition, and holds also for rigidly rotating neutron stars (Zdunik et al. 2006).

An important global parameter for hydrostatic equilibrium configurations is their baryon mass, $M_{\rm b}$. It is defined as the baryon number of the star, $A_{\rm b}$, multiplied by the "mass of a baryon", m_0, defined as $1/56$ of the mass of the ^{56}Fe atom: $m_0 = 1.6586 \times 10^{-24}$ g. During evolution of an isolated neutron star, including the phase transitions in its interior, $M_{\rm b}$ remains strictly constant.

We define the equatorial radius of an axisymmetric neutron star as the proper length of the equator divided by 2π. Examples of $M_{\rm b}$–$R_{\rm eq}$ curves for non-rotating and rotating neutron stars without a phase transition $\{C\}$, with a weak first-order phase transition $\{C^\star_{\rm weak}\}$, and a strong first-order phase transition $\{C^\star_{\rm strong}\}$, are shown in Fig. 1. Dotted segments correspond to unstable configurations (instability with respect to the axisymmetric perturbations). As one sees, fast rotation significantly changes the $M_{\rm b}(R_{\rm eq})$ dependence, e.g., by increasing the mass and the radius of the configuration with $P_{\rm c} = P_0$ denoted by C_0.

General relations between models calculated for three types of the EOS can be formulated. At a given $M_{\rm b}$, $R_{\rm eq}(C^\star_{\rm strong}) < R_{\rm eq}(C^\star_{\rm weak}) < R_{\rm eq}(C)$. Moreover, maximum allowable baryon masses satisfy $M_{\rm b,max}(C^\star_{\rm strong}) < M_{\rm b,max}(C^\star_{\rm weak}) < M_{\rm b,max}(C)$; the
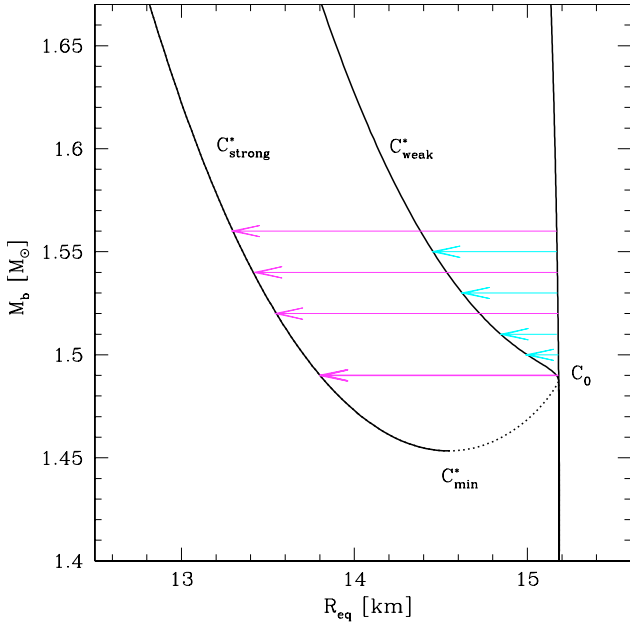
Fig. 2. Zoomed fragment of Fig. 1, in the vicinity of the phase transition. For other explanations see the text.

Fig. 3. Transition from a one-phase configuration C with a meta-stable core of radius r_N to a two-phase configuration $C^\star$ with a S-phase core with a radius r_S. These two configurations have the same baryon mass $M_b = M_b^\star$ and total angular momentum $J = J^\star$. Notice that in contrast to the case of a first order phase transition with $\lambda < \lambda_{crit}$ studied in Zdunik et al. (2007, see Fig. 2 of that paper), here r_N is much smaller than r_S (in the limiting case $r_N = 0$ while r_S is sizeable).

same inequalities are valid for maximum allowable gravitational mass, M_{max}.

Differences in the mass-radius behavior are most pronounced in the vicinity of configuration C_0, with $P_c = P_0$. This region, bounded by a rectangle in Fig. 1, is shown in Fig. 2, where the arrows connect configurations with same M_b. For simplicity, we first consider non-rotating stars. For $\lambda < \lambda_{crit}$, configurations with $P_c > P_0$ form a monotonous branch $C_{weak}^\star$. For $\lambda > \lambda_{crit}$, a segment with $P_0 < P_c < P_{c,min}^\star$ consists of configurations $C_{strong}^\star$ with $dM^\star/d\rho_c^\star < 0$, which are therefore unstable with respect to radial perturbations. Therefore, for $\lambda > \lambda_{crit}$ the stable branches $\{C\}$ and $\{C^\star\}$ are disjoint. In both cases ("weak" and "strong"), the central density jumps from ρ_N to ρ_S when passing from the C branch to the $C^\star$ branch. All these properties were derived a long time ago for non-rotating neutron stars. Recently it has been shown that they hold also for phase transitions in rigidly rotating neutrons stars when the stationary axially symmetric families C and $C^\star$ contain configurations of a fixed stellar angular momentum J (Zdunik et al. 2006). The standard non-rotating case corresponds to $J = 0$.

3. Calculation of the energy release

We restrict ourselves to axially symmetric, rigidly rotating neutron stars in hydrostatic equilibrium. In what follows, by "radius" we mean the equatorial circumferential radius, R_{eq}.

We assume that at a central pressure $P_c = P_{nucl}$ the nucleation of the S phase in an overcompressed core, of a small radius r_N (of configuration C) initiates a strong first-order phase transition. This leads to formation of a large S-phase core of radius r_S in a new configuration C^*, as shown in Fig. 3.

We compare the hydrostatic equilibria of neutron stars corresponding to the EOSs with and without the phase transition using the numerical library LORENE (http://www.lorene.obspm.fr), obtaining the axisymmetric, rigidly rotating solutions of Einstein equations as in Zdunik et al. (2007). The accuracy of the solution, measured
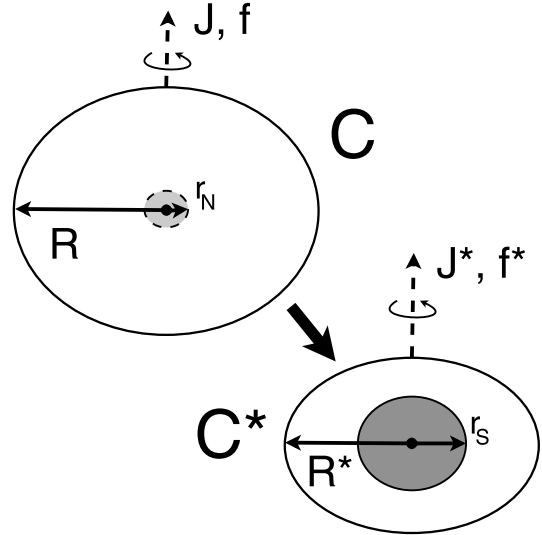
with the general relativistic virial theorem (Gourgoulhon & Bonazzola 1994), is typically 10^{-6}.

The neutron-star models can be labeled by the central pressure P_c (central density is not continuous) and rotational frequency $f = \Omega/2\pi$. These parameters are natural from the point of view of numerical calculations. But we can introduce another parametrization, more useful for other purposes. In order to study the stability of rotating stars, a better choice is the central pressure, P_c, and the total angular momentum of the star, J.

We additionally assume that the transition of the star from a one-phase configuration to the configuration with a dense core of the S-phase takes place at fixed baryon mass M_b (no matter ejection) and fixed total angular momentum of the star J (loss of J due to the electromagnetic or gravitational radiation is neglected). The energy release during transition $C(M_b, f) \longrightarrow C^\star(M_b, f^\star)$ is therefore calculated from the change of the stellar mass-energy during this process,

$$E_{rel} = c^2 \left[M(C) - M(C^\star) \right]_{M_b, J}. \tag{1}$$

The precision of the determination of E_{rel} depends on the numerical accuracy of calculations of the configurations with the same J and M_b. Taking into account that E_{rel} is $3 \div 4$ orders of magnitude smaller than M (for the overpressures ranging from a few to 20 percent) this precision is typically better than 1%.

3.1. Energy release for polytropic EOSs

The use of the polytropic EOSs for the N and S phases not only guarantees very high precision of numerical calculation, but also opens the possibility of the exploration of a wide region of the parameter space. A description of the polytropic EOSs and their application to relativistic stars with phase transitions was presented in detail in our previous publications in this series (Bejger et al. 2005; Zdunik et al. 2006).
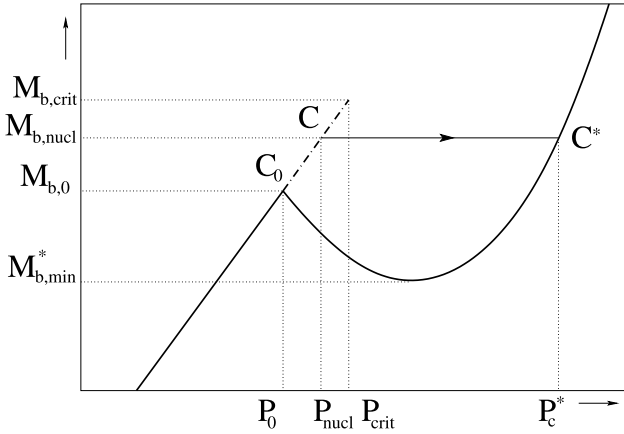
Fig. 4. Total baryon mass M_b of hydrostatic stellar configuration, versus central pressure P_c, at fixed stellar angular momentum J. The solid line denotes stable states, dash-dot line - the states that are metastable with respect to the N $\longrightarrow$ S transition. For a central pressure P_{nucl} the S-phase nucleates in the super-compressed core of configuration C, and this results in a transition $C \longrightarrow C^*$ into a stable configuration with a S-phase core and central pressure P_c^*. Both configurations C and C^* have the same baryon mass M_b.

Table 1. The parameters of the polytropic EOSs.

EOS	K_S (erg cm^{-3})	γ_S	λ	λ_n
PolW	5.11×10^{11}	3.5	1.44	1.4
PolS1	1.602×10^{11}	4	1.66	1.6
PolS2	1.257×10^{11}	4	1.77	1.7

Parameters of our EOS models are collected in Table 1. The basic EOS for the N phase, named PolN, is $P = K_N c^2 (n_b/n_1)^{\gamma_N}$, where $n_1 = 0.1$ fm^{-3} and $K_N = 4.15 \times 10^{12}$ erg cm^{-3}, and $\gamma_N = 2.5$. Construction of the EOS for the S-phase and of the first order phase transition at $P = P_0$ is based on Appendix A of Zdunik et al. (2006). The transition point is the same for all three EOSs, and is defined by $P_0 = 3.686 \times 10^{34}$ erg cm^{-3}, $n_N = 0.25$ fm^{-3}, and $\rho_N = 4.42 \times 10^{14}$ g cm^{-3}. The density jump corresponding to the phase transition is defined by the parameters $\lambda = \rho_S/\rho_N$ and $\lambda_n = n_S/n_N$, connected by the relation $\lambda = 1 + (\lambda_n - 1)(1 + P_0/\rho_N c^2)$. The S-phase EOS is a polytrope with the parameters K_s and γ_s. The non-rotating reference configuration C_0 has $M = M_0 = 1.38\, M_\odot$ and $R = R_0 = 15.2$ km. The phase transition in PolW1 is *weak* ($\lambda < \lambda_{crit}$), while those in PolS1 and PolS2 are *strong* ($\lambda > \lambda_{crit}$).

In Fig. 5 we present the energy release as a function of $\bar{r}_s = r_s/R(C)$, for several values of the angular momentum of the metastable configurations $C(J)$. As we see, the energy release corresponding to a given value of $\bar{r}_s$ depends rather strongly on the total angular momentum. For example, the value of E_{rel} at $\bar{r}_s = 0.41$, for $J = 1.0\, GM_\odot^2/c$, is twice that for $J = 0$ (nonrotating star). Moreover, the value of E_{rel} for minimum $\bar{r}_s$ (at fixed J) is (nearly) independent of J. This reflects the independence of $E_{rel}(\delta \bar{P} = 0)$ from J.

In Fig. 6 we present the energy release as a function of the overpressure of the metastable N phase in the center of the metastable star $C(M_b, J)$, for several values of J. The value of P_{nucl} (or $\delta \bar{P}$) can be determined from microscopic considerations, combined with physical conditions prevailing at the star center as well as with the evolution rate. Having determined P_{nucl}, we can determine the energy release, E_{rel}, due to
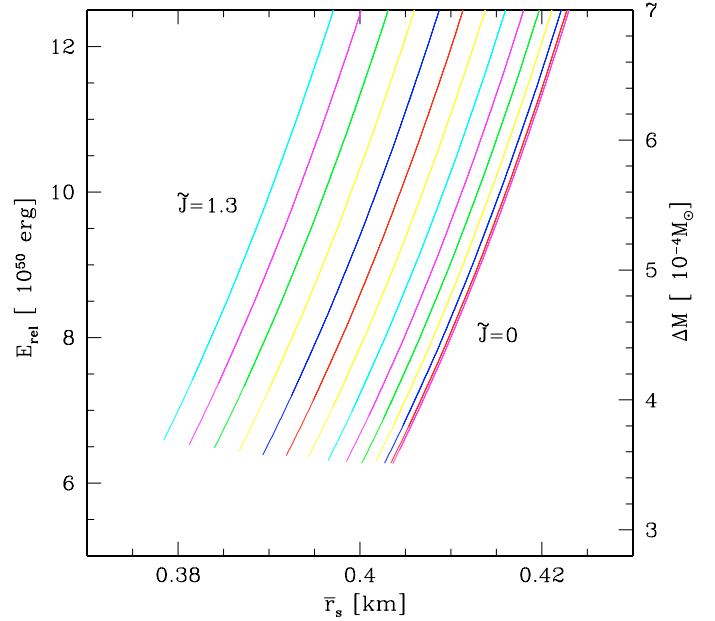

Fig. 5. (Color online) The energy release due to the core-quake of a rotating neutron star as a function of the dimensionless equatorial radius of the S-phase core, $\bar{r}_s$. Calculations are performed for the EOS PolS1 from Table 1. Different curves correspond to the different values of the total angular momentum of rotating star, fixed along each curve, $J = \widetilde{J}\, GM_\odot^2/c = (0, 0.1, \ldots, 1.3) \times GM_\odot^2/c$, from the right-most curve to the left-most curve.

the core-quake $C(M_b, J) \longrightarrow C^\star(M_b, J)$, where the metastable one-phase configuration, and the final two-phase configuration, have the same values of the baryon mass M_b and total angular momentum J.

As we see in Fig. 6, the energy release in a collapse of a rotating star is nearly independent of the angular momentum of the collapsing configuration, and depends exclusively on the degree of metastability of the N phase at the stellar center (departure of matter from chemical equilibrium), measured by the overpressure $\delta \bar{P}$. Consequently, to obtain the energy release associated with a core-quake of a rotating neutron star, it is sufficient to know the value of E_{rel} for a non-rotating star of the same central overpressure. More detailed analysis of the dependence of E_{rel} on the rotation of the star leads to the conclusions that although this effect is very small (of the order of 1%) it is systematic, as visualized in Fig. 7.

The configurations $C(M_b, J)$ and $C^\star(M_b, J)$, considered in this section, are the fast rotating ones; those with largest J are close to the Keplerian (mass shedding) limit. This is visualized in Fig. 8, where we plot the oblateness of the star and the kinetic to potential energy ratio. And still, in spite of the fast rotation and high oblateness, the energy release is the same as in a non-rotating star of the same initial central overpressure.

Thus, the remarkable independence of E_{rel} from J, obtained in Zdunik et al. (2007) for $\lambda < \lambda_{crit}$, when the small-core approximations were valid, holds also for $\lambda > \lambda_{crit}$, where perturbative arguments cannot be used.

3.2. Realistic EOS – an example

Here, we check the general validity of results obtained for a polytropic EOS discussed in Sect. 3.1 by performing numerical calculations for realistic EOSs with a strong first-order phase transition. For the EOS of the crust we took the model of
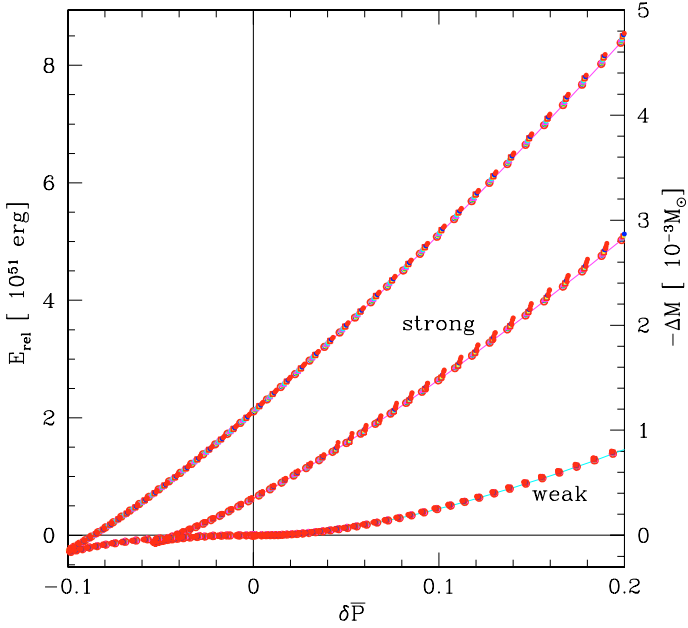
Fig. 6. (Color online) The energy release due to the mini-collapse of a rotating neutron star as a function of the overpressure $\delta\overline{P}$ of the N phase of the matter in the center of the star, for three EOSs from Table 1. The *bottom curve* is calculated for the PolW EOS with a weak first-order phase transition, so that $E_{rel}(0) = 0$. The *middle curve* and the *top curve* are for the PolS1 and PolS2 EOSs, respectively, with strong first-order phase transitions. The points of different color correspond to the different values of total angular momentum of the rotating star, $J = \widetilde{J}\,GM_\odot^2/c = (0, 0.1, \ldots, 1.3) \times GM_\odot^2/c$. For a given EOS, results for all rotating configurations can be very well approximated by a single curve, independent of J.

Fig. 8. *Top panel*: the ratio of polar radial coordinate to the equatorial radial coordinate ratio. *Bottom panel*: the ratio of the kinetic energy, T and the absolute value of the potential energy, W, for the reference stellar configurations (central pressure P_0, Table 1) consisting of the N phase of dense matter, described by the polytropic EOS, PolN, of Table 1. Large dots correspond to the values of the total stellar angular momentum, $J = \widetilde{J}GM_\odot^2/c = (0.1, \ldots, 1.5) \times GM_\odot^2/c$, which were used in Figs. 5, 6.
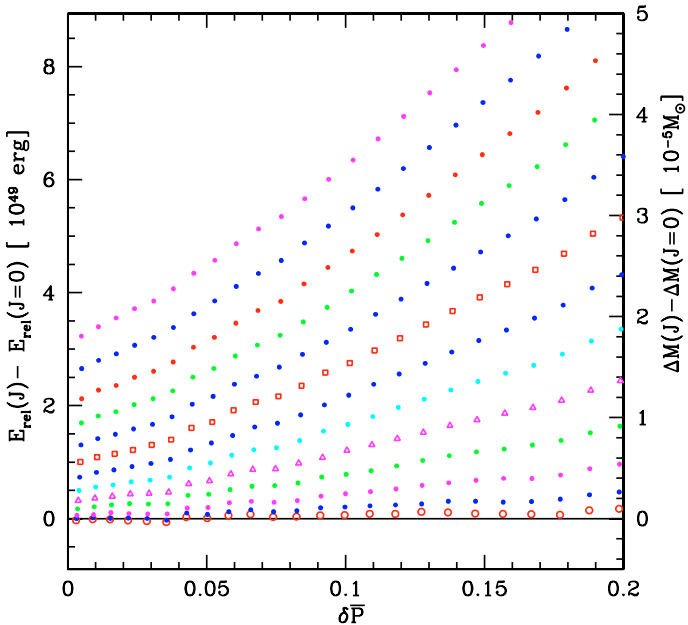

Fig. 7. (Color online) The difference between the energy release due to the mini-collapse of a rotating neutron star and a non-rotating one as a function of the overpressure $\delta\overline{P}$ for the PolS1 EOS (the *middle curve* in Fig. 6). The points of different color correspond to the different values of total angular momentum of the rotating star, $J = \widetilde{J}\,GM_\odot^2/c = (0, 0.1, \ldots, 1.3) \times GM_\odot^2/c$ from *bottom* to *top*. Note the two orders of magnitude difference in the scale of the vertical axis in this figure and Fig. 6.
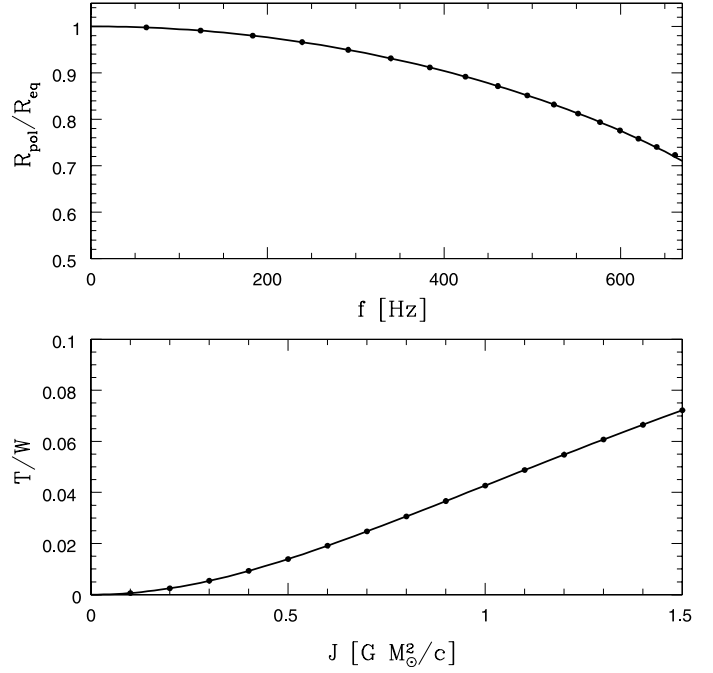
Douchin & Haensel (2001). The constituents of the N phase of the core were neutrons, protons, electrons, and muons. The nucleon component was described using the relativistic mean-field model with scalar self-coupling constructed by Zimanyi & Moszkowski (1990). The values of the meson-nucleon coupling constants are $g_\sigma/m_\sigma = 3.122$ fm, $g_\omega/m_\omega = 2.1954$ fm, $g_\rho/m_\rho = 2.1888$ fm. The dimensionless coefficients in the cubic and quartic terms in scalar self-coupling are $b = -6.418 \times 10^{-3}$ and $c = 2.968 \times 10^{-3}$, respectively. As an example of the S-phase we considered the kaon-condensed matter. We constructed a specific dense matter model with a strong first-order N $\longrightarrow$ S transition implied by kaon condensation. Coupling of kaons to nucleons is described by the model of Glendenning & Schaffner-Bielich (1999), with $U_K^{\rm lin} = -115$ MeV. The resulting EOS is shown in Fig. 9. The phase transition is the *strong* one, with $\lambda > \lambda_{\rm crit}$ (see the caption of Fig. 9). The EOS with kaon condensation that we selected is an example of an EOS with a strong first order phase transition. It was used to check our theory on a concrete model of a dense exotic core and using a realistic description of the neutron star crust. However, the true character the phase transition if it occurs in neutron star cores (strong or weak first order, or perhaps second order) cannot be reliably predicted because of the uncertainties in the theory of matter at supranuclear density (see, e.g., Zuo et al. (2004); Li et al. (2006) and references therein).

In Fig. 10 we show the energy release due to the $C(M_{\rm b}, J) \longrightarrow C^\star(M_{\rm b}, J)$ transition, versus overpressure. The values obtained for different values of J are marked with different colors and symbols. To an even better approximation than for the polytropic models, all color points lie along the same line. For a given overpressure $\delta\overline{P}$, the energy release does not
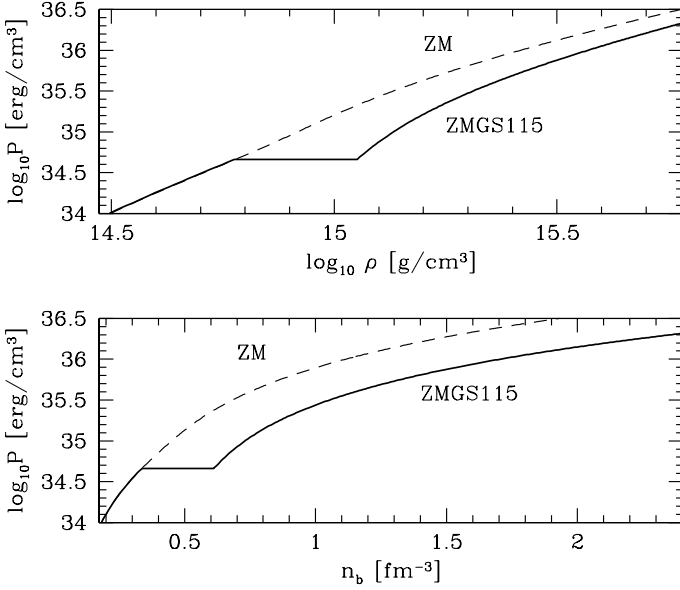
Fig. 9. EOS with first-order phase transition due to kaon condensation described and used in Sect. 3.2. in the present paper. The phase transition occurs at $P_0 = 4.604 \times 10^{34}$ erg cm^{-3}. On the N-phase side, $n_N = 0.3375$ fm^{-3} and $\rho_N = 5.973 \times 10^{14}$ g cm^{-3}. On the kaon-condensed S-side, $n_S = 0.6122$ fm^{-3} and $\rho_N = 1.125 \times 10^{15}$ g cm^{-3}. Therefore, $\lambda = \rho_S/\rho_N = 1.884$, which is greater than $\lambda_{\rm crit} = \frac{3}{2}(1 + P_0/\rho_N c^2) = 1.629$.

depend on J of collapsing metastable configuration. This property holds for a broad range of of stellar angular momentum, $J = (0.1, \ldots, 1.0) \times GM_\odot^2/c$.

4. Decomposition of the energy release

As was already said, we restrict ourselves to the stationary, axisymmetric states of rotating neutron stars. In the Newtonian theory, the energy of a rigidly rotating axially symmetric star (body) is easily decomposed into kinetic energy of rotation, T, and internal energy, U, which is the total energy of the star measured in the stellar (body) reference system. The kinetic energy of rotation is $T = \frac{1}{2}J\Omega = \frac{1}{2}I\Omega^2$, where the moment of inertia $I = J/\Omega$. On the other hand, the total energy measured in "the laboratory frame", E, is related to U by $U = E - J\Omega$. For a rigid rotation $U = E - \frac{1}{2}J\Omega$.

In general relativity, all kinds of energies sum to give the stellar gravitational mass, $M = E/c^2$, which is the source of the space-time curvature. Therefore, the decomposition of Mc^2 into T and U is ambiguous. Here, we will use a standard Newtonian-like formula, $T = \frac{1}{2}J\Omega$, where both J and Ω are well defined quantities (Friedman et al. 1986).

The transition $C(M_b, J) \longrightarrow C^\star(M_b, J)$ is accompanied by spin-up of the neutron star, and an increase of its kinetic energy. Our results show that while $E_{\rm rel}$ is to a very good approximation independent of J, the kinetic energy increase $\Delta T \equiv (T^\star - T)_{M_b, J} = \frac{1}{2}J(\Omega^\star - \Omega)_{M_b, J}$ grows rapidly with J. This is seen in Fig. 10. The contribution to the energy release resulting from the decrease of the internal energy of the star will be denoted by $E_{\rm rel}^{\rm (int)}$. It is given by

$$E_{\rm rel}^{\rm (int)}(\delta\overline{P}, J) = \frac{1}{2}J(\Omega^\star - \Omega)_{M_b, J} + E_{\rm rel}(\delta\overline{P}). \quad (2)$$

Therefore, the energy release in the star reference system is greater than the total energy release measured by a distant observer. The difference increases rapidly with J, see Fig. 10.
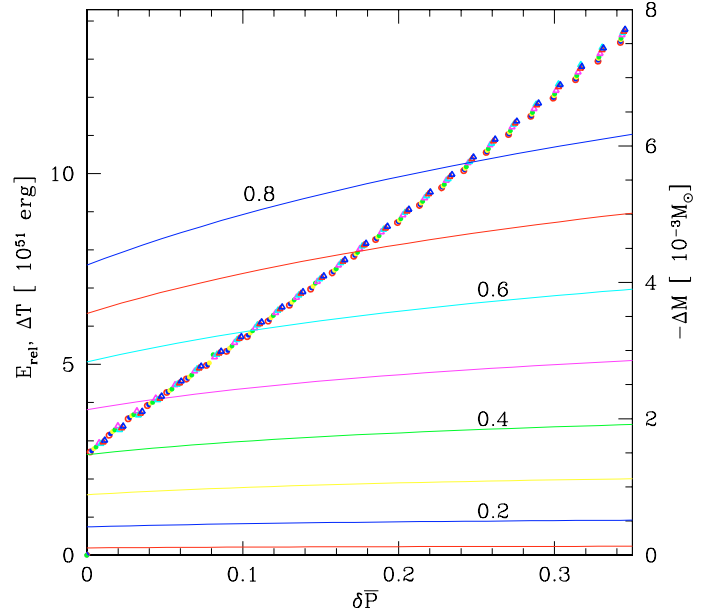

Fig. 10. (Color online) The total energy release, $E_{\rm rel}$, due to the collapse of a rotating neutron star, implied by kaon condensation, as a function of the metastability (overpressure) of the normal phase of the matter in the center of the star for the EOS in Fig. 9. The points of different color correspond to the different values of total angular momentum of the rotating star. The results for all rotating configurations can be very well approximated by one curve. Solid lines: kinetic energy increase, $\Delta T = T^\star - T$, for fixed values of $J = \widetilde{J}GM_\odot^2/c = (0.1, \ldots, 0.8) \times GM_\odot^2/c$. The bottom line is for $\widetilde{J} = 0.1$, and top line for $\widetilde{J} = 0.8$. Note the different definition of the sign of $E_{\rm rel} = (M - M^\star)c^2$ and $\Delta T = T^\star - T$.

5. Phase transition associated with overcoming the energy barrier

In the case of a strong first-order phase transition, configurations with $P_{\rm crit} > P_c > P_0$ are not the only ones that are metastable with respect to the N $\longrightarrow$ S transition. In order to look for additional metastable N-phase configurations we plotted, in Fig. 11, the vicinity of the reference configuration C_0 in the $M_b - R$ plane: for $M_b(C_0) > M_b > M_b(C_{\rm min}^\star)$ we have three equilibrium configurations with a given M_b. Consider a triplet of equilibrium configurations $C_1 C_1^{\star\prime} C_1^\star$. Two of them, C_1 and $C_1^\star$, are stable (local minimum of energy), and one, $C_1^{\star\prime}$, is unstable (local maximum of energy). Notice that the N-phase configurations in the $C_0 C_{\rm min}$ segment are characterized by a *negative* overpressure (which might then be called "underpressure") $\delta\overline{P} = P_{\rm nucl}/P_0 - 1 < 0$.

In Fig. 11 we indicated, with horizontal lines, several examples of transitions between equilibrium configurations with the same M_b. To understand the nature of these transitions, we plotted in Fig. 12 the energy release, Eq. (1), associated with a transition between a pair of configurations, versus the *negative* overpressure. We see that the functional dependence $E_{\rm rel}(\delta\overline{P})$, together with (a quite precise) independence from J, continue smoothly into the region of negative $\delta\overline{P}$. Notice that point A in Fig. 12 corresponds to $C_0 \longrightarrow C_0^\star$. As far as the transitions $C_1 \longrightarrow C_1^{\star\prime}$ (segment BD in Fig. 12) are concerned, they are always associated with $E_{\rm rel} < 0$, i.e. to make them, the star should gain (absorb) energy instead of releasing it. The necessary energy input is $\mathcal{B} = |E_{\rm rel}|$, and it reaches a maximum at point D, corresponding to $C_{\rm min} \longrightarrow C_{\rm min}^\star$. Therefore, in order to get to $C_1^{\star\prime}$ by forming a small S-phase core, the system has to overcome the energy barrier. Then, configuration $C_1^{\star\prime}$ (which is unstable) can
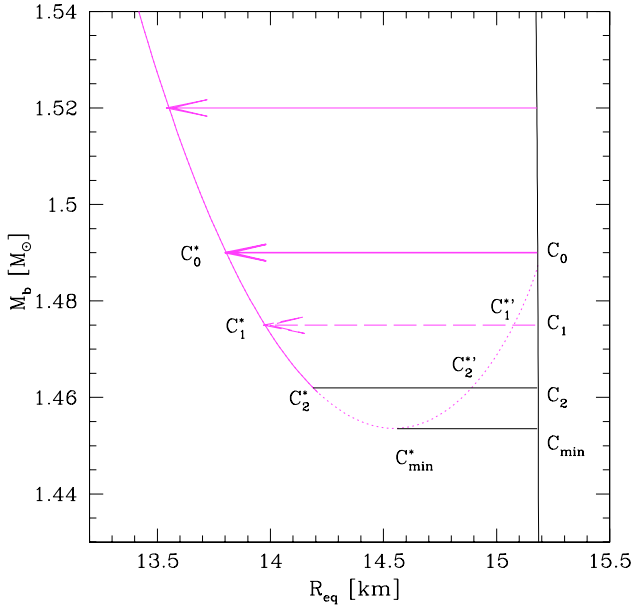
Fig. 11. Three families of neutron stars in the $M_b - R_{eq}$ plane and the transition $C_1 \longrightarrow C_1^\star$ via overcoming the energy barrier.
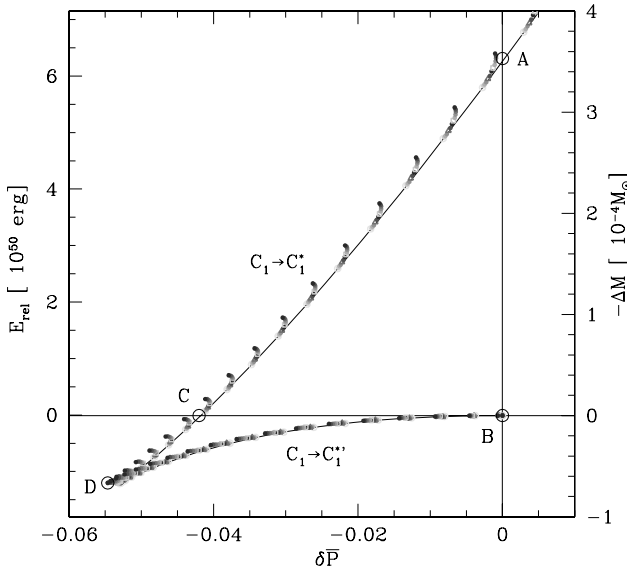

Fig. 12. (Color online) Energy release, Eq. (1), versus overpressure $\delta\overline{P} = (P_c - P_0)/P_0$, for transitions $C_1 \longrightarrow C_1^\star$ and $C_1 \longrightarrow C_1^{\star\prime}$ visualized in the $M_b - R$ plane in Fig. 11. Points of different color correspond to transitions with different angular momentum $J = \widetilde{J}GM_\odot^2/c^2 = (0, 0.1, \ldots, 0.9) \times GM_\odot^2/c^2$. Solid line – results for $J = 0$ (non-rotating stars). Point A corresponds to $C_0 \longrightarrow C_0^\star$. Point B corresponds to $C_0 \longrightarrow C_0^{\star\prime} = C_0$, point D to $C_{min} \longrightarrow C_{min}^\star$, and point C to $C_2 \longrightarrow C_2^\star$.

collapse into $C_1^\star$ with a large core, and this collapse is associated with an energy release. In this way the star reaches the global minimum of M at fixed M_b. However, this is the case provided the transition takes place above the horizontal line $C_2 C_2^\star$.

Thus, N-phase configurations in the $C_0 C_2$ segment are metastable with respect to the transition to large S-phase core configuration in the $C_0^\star C_2^\star$ segment. However, such a transition requires overcoming the energy barrier of height $\mathcal{B}$. Consider a specific example with $\delta\overline{P} = -0.02$. Using Fig. 12, we see that $\mathcal{B} \sim 10^{49}$ erg while $E_{rel} = 3 \times 10^{50}$ erg. Generally, for this model of phase transition we have $E_{rel} \gg \mathcal{B}$ for underpressures

$\delta\overline{P} > -0.03$. The excitation energy, E_{exc}, contained in radial pulsations, scales as the square of relative amplitude $\delta R/R$. For the fundamental mode, $E_{exc} \approx 10^{53}(\delta R/R)^2$ erg. Therefore, E_{exc} exceeds 10^{49} erg as soon as $\delta R/R > 0.01$, a condition that is easy to satisfy by an newly born neutron star.

However, a second obstacle for the collapse of the configuration with a negative $\delta\overline{P}$ should be pointed out. Apart from the energy condition allowing overcoming an energy barrier, there is a timescale condition: there should be enough time to form the S-phase core. This latter condition may be more difficult to fulfill than the former one, particularly if there is a need to create strangeness, as in kaon condensation or in the formation of three-flavor u-d-s quark matter from a deconfined two-flavor (u-d) state. Once again, favorable conditions for $C_1 \longrightarrow C_1^\star$ with overcoming $C_1^{\star\prime}$ could exist in a newborn neutron star. A neutron star born in gravitational collapse not only pulsates, with a pulsational energy much greater than $\mathcal{B}$, but additionally a high temperature $\sim 10^{11}$ K in the stellar core can allow for a rapid nucleation of the S-phase.

6. Discussion and conclusions

The most important result of the present paper is that the total energy release, associated with a *strong* first-order phase transition at the center of a rotating neutron star, depends only on the overpressure at the center of the metastable configuration and is nearly *independent of the star rotation rate*. This result holds even for fast stellar rotation, when the star shape deviates significantly from sphericity, and for overpressures as high as (10–20)%. This property is of great practical importance. It implies that the calculation of the energy release for a given overpressure, requiring very high precision 2D calculations to guarantee $M_b = M_b^\star$, can be replaced by a simple calculation of non-rotating spherical stars. The independence of the energy release of the rotation should be treated as a result of numerical calculations and is subject to the numerical accuracy of the stellar parameter determination. Strictly speaking our numerical results indicate that, if the energy release depends on the rotation, this dependence is extremely weak and the maximum deviation from the nonrotating value for a given overpressure is of the order of 1%.

We studied the stability of configurations with a central pressure below that for the equilibrium phase transition. If the initial state of the neutron star is excited, e.g. it is pulsating, then the formation of a large dense phase core is possible, but it requires climbing over the energy barrier associated with formation of a small core. The excitation energy has to be greater than the height of the energy barrier. Additionally, if a phase transition is connected with the change of strangeness per baryon, then the temperature has to be high enough to make strangeness production sufficiently rapid. Such conditions might be realized in the cores of newly born neutron stars.

Note that the energy release $E_{rel} \sim 10^{51}-10^{52}$ erg is an absolute upper bound on the energy that can be released as a result of a phase transition at the star center. The energy ΔE can be shared between, e.g., stellar pulsations, gravitational radiation, heating of the stellar interior, X-ray emission from the neutron star surface, and even a gamma-ray burst.

References

Bejger, M., Haensel, P., & Zdunik, J. L. 2005, MNRAS, 359, 699
Berezhiani, Z., Bombaci, I., Drago, A., Frontera, F., & Lavagno, A. 2003, ApJ, 568, 1250
Berezin, Yu. A., Dmitrieva, O. E., & Yanenko, N. N. 1982, Pisma v Astron. Zh., 8, 86
Berezin, Yu. A., Mukanova, B. G., & Fedoruk, M. N. 1983, Pisma v Astron. Zh., 9, 116
Diaz Alonso, J. 1983, A&A, 125, 287
Douchin, F., & Haensel, P. 2001, A&A, 380, 151
Friedman, J. L., Ipser, J. R., & Parker, L. 1986, ApJ, 304, 115
Glendenning, N. K. 2000, Compact Stars. Nuclear Physics, Particle Physics, and General Relativity (Berlin: Springer)
Glendenning, N. K., & Schaffner-Bielich, J. 1999, Phys. Rev. C, 60, 025803
Gourgoulhon, E., & Bonazzola, S. 1994, Class. Quantum Grav., 11, 443
Haensel, P., & Prószyński, M. 1980, Phys. Lett., 96B, 233
Haensel, P., & Prószyński, M. 1982, ApJ, 258, 306
Haensel, P., & Schaeffer, R. 1982, Nucl. Phys. A, 381, 519
Haensel, P., Zdunik, J. L., & Schaeffer, R. 1986, A&A, 160, 251
Haensel, P., Denissov, A., & Popov, S. 1990, A&A, 240, 78
Haensel, P., Potekhin, A. Y., & Yakovlev, D. G. 2007, Neutron Stars 1, Equation of State and Structure (New York: Springer)
Iida, K., & Sato, K. 1997, Prog. Theor. Phys., 98, 277
Iida, K., & Sato, K. 1998, Phys. Rev. C., 58, 2538
Kaempfer, B. 1981, Phys. Lett. 101B, 366
Kaempfer, B. 1982, Astron. Nachr., 303, 231
Li, A., Burgio, G. F., Lombardo, U., & Zuo, W. 2006, Phys. Rev. C, 74, 055801
Migdal, A. B., Chernoutsan, A. I., & Mishustin, I. N. 1979, Phys. Lett. 52B, 172
Muto, T., & Tatsumi, T. 1990, Prog. Theor. Phys., 83, 499
Norsen, T. 2002, Phys. Rev. C, 65, 045805
Seidov, Z. F. 1971, Sov. Astron.- Astron. Zh., 15, 347
Weber, F. 1999, Pulsars as Astrophysical Laboratories for Nuclear and Particle Physics (Bristol & Philadelphia: IoP Publishing)
Zdunik, J. L., Haensel, P., & Schaeffer, R. 1987, A&A, 172, 95
Zdunik, J. L., Bejger, M., Haensel, P., & Gourgoulhon, E. 2006, A&A, 450, 747
Zdunik, J. L., Bejger, M., Haensel, P., & Gourgoulhon, E. 2007, A&A, 465, 533
Zimanyi, J., & Moszkowski, S. A. 1990, Phys. Rev. C, 42, 1416
Zuo, W., Li, A., Li, Z. H., & Lombardo, U. 2004, Phys. Rev. C, 70, 055802